JTTEE5 18:563–571
DOI: 10.1007/s11666-009-9375-5
1059-9630/$19.00 © ASM International

Properties of Reactive Plasma Sprayed TiB_2-$TiC_{0.3}N_{0.7}$ Based Composite Coatings with Cr Addition and Laser Surface Treatment

Zhengping Mao, Jun Wang, Baode Sun, and Chengwu Yao

(Submitted May 7, 2009; in revised form June 22, 2009)

Thick TiB_2-$TiC_{0.3}N_{0.7}$ based composite coatings were deposited by reactive plasma spraying (RPS) successfully in air. The influence to the coating properties (morphology, Vickers microhardness and corrosion resistant property) with Cr addition in the thermal spray powder and TiB_2-$TiC_{0.3}N_{0.7}$ based coatings treated by laser were investigated. The phase composition, structure and properties of composite coatings were studied using XRD, SEM, EDS, Vickers microhardness and electrochemical testers. The results show that the Vickers microhardness values and the density of laser surface treated coatings are improved significantly. The Cr addition in the thermal spray powder can increase the density, improve the wettability of ceramic phases, uniform the phase distribution and enhance the corrosion-resistant property of coatings. However, due to lower microhardness of metal Cr than ceramic phases in coatings, the Vickers microhardness values of plasma sprayed coatings and plasma sprayed coatings with laser surface treatment are a little lower than that of each coating without Cr addition in the thermal spray powder.

Keywords composite coating, laser surface treatment, polarization curve, reactive plasma spraying, Vickers microhardness

1. Introduction

Ceramic-based coatings deposited in situ with high microhardness, superior corrosion and wear resistance have been widely studied recently (Ref 1-3). The in situ formation technology permits to obtain high bonding strength and clean interface of reinforcement phases without contamination in coatings (Ref 4, 5). Reactive thermal spraying, which combines the in situ technology and thermal spraying method, has been used to successfully deposit the ceramic-based coating (Ref 6). Hard ceramic phases (carbides, borides and nitrides) are formed in situ by the reactions between the injected powder and the carrier gas during spraying (Ref 7-9). However, the ceramic phases in this study were formed by the reactions between the injected powders, and the powder with N_2 in air during the course of plasma spraying.

TiB_2 and Ti(C, N) coatings, which possess outstanding hardness, high wear resistance, good stability at high temperature (Ref 10, 11) and good chemical stability (Ref 12), have been used to improve the tool life in industry (Ref 1). Cermet coatings, which combine the toughness of metals and the hardness of ceramic phases, have been investigated extensively in industry such as petroleum, chemical and wear resistant in hot galvanizing (Ref 13, 14). Metal Cr and Co, as metallic binder in ceramic coatings, can make the cermet coating well bond with the substrate, obtaining the coatings with low porosity and good wetting property between ceramic phases (Ref 15, 16).

The properties of thermal sprayed coatings can be improved significantly with laser surface treatment (Ref 17, 18). The wear resistance of plasma sprayed Ni-Cr-B-Si+WC coating with laser processing was much better than that of plasma sprayed coating (Ref 17). Furthermore, the corrosion resistance of plasma sprayed Ni-coated WC with laser remelting was better than that of as-sprayed coating and post-heating treatment coating (Ref 18). In the present study, thick TiB_2-$TiC_{0.3}N_{0.7}$ based composite coatings were prepared by RPS successfully. The reactive plasma sprayed coatings were processed by laser to investigate its action mechanics. In addition, the effect to the morphology, microhardness and corrosion resistance property of coatings with Cr addition in the thermal spray powder was studied.

2. Experimental Details

2.1 Preparation of Thermal Spray Powder

Commercial Ti powder with particle size from 45 to 70 μm (Jin Jiang Metallic Powder Co. Ltd., Shanghai,

Zhengping Mao, Jun Wang, Baode Sun, and **Chengwu Yao**, State Key Laboratory of Metal Matrix Composites, Shanghai Jiaotong University, Shanghai 200240, P.R. China. Contact e-mail: junwang@sjtu.edu.cn.

P.R. China) and B_4C powder with particle size from 30 to 50 μm (Sinopharm Chemical Reagent Co. Ltd., Shanghai, P.R. China) were used as starting material for RPS. Furthermore, NiCoCrAlY powder and the blended powder of Cr and NiCoCrAlY (General Research Institute for Nonferrous Metals, Beijing, P.R. China) with particle size from 45 to 70 μm were added to thermal spray powder (Ti-Cr-B_4C) as metallic binder, respectively. The purity of Ti, Cr and B_4C powder is more than 99, 99 and 90%, respectively. The composition of NiCoCrAlY powder is 22 wt.% Co, 17 wt.% Cr, 12.5 wt.% Al, 0.6 wt.% Y and balance Ni.

In order to obtain well-proportioned powder, Ti, Cr and B_4C powders were mixed by ball milling for 40 h before slurry preparation for spray-drying. The weight ratio of Ti:Cr:B_4C is about 4.1:1:1.6. The slurry, which consists of disperser, bond, Ti, Cr and B_4C powders, was prepared prior to spray-drying. The addition of disperser (A15) and bond (PVA) are 0.5 and 2.5 wt.% of the solid powder, respectively. The solid loading of the slurry is 35 wt.%. The import and export temperatures of the spray-dried equipment (Da Chuan Spray-drying Co. Ltd., Shanghai, P.R. China) are 250 and 110 °C, respectively. Then, composition A, which contains 25 wt.% NiCoCrAlY and 75 wt.% spray-dried Ti-Cr-B_4C powder (45-70 μm), was used for one deposition. Composition B, which contains 15 wt.% Cr and 25 wt.% NiCoCrAlY as well as 60 wt.% spray-dried Ti-Cr-B_4C powder (45-70 μm), was used for another deposition. Both of the blended powders were stirred by electric blender of JB90-D (Shanghai, P.R. China) for an hour before coating deposition.

2.2 Preparation of Samples and Coatings

Medium carbon steel (0.42-0.50 wt.% C steel) with 40 mm diameter and thickness of 3 mm was used as the substrate material. After finally polished to 400 mesh abrasive paper, the substrates were grit-blasted with alumina to get the fresh surface, ultrasonically cleaned in anhydrous ethanol, and then dried in air prior to coating deposition. The blended powder was selected as feedstock of the top coating. Argon was selected as carrier gas. The coatings were deposited in air. Buffer layer of NiCoCrAlY coating (~100 μm in thickness) was selected for adjusting the mismatch of thermal expansion coefficient (CTE) between the substrate and the top coating. The experimental facility for coating deposition is XM-80 plasma spraying facility (Shanghai, P.R. China). The detailed spraying parameters are shown in Table 1.

Table 1 RPS spraying parameters

Spraying parameters	Bond coating	Top coating
Current, A	550	600
Voltage, V	60	60
Spraying distance, mm	100	100
Powder feed rate (Ar), g/min	10	15

2.3 Laser Surface Treatment, Microstructure and Microhardness of Coatings

The laser surface treatment for reactive plasma sprayed coatings was performed using a TRUMPF PF CO_2 laser (Germany) with 6.5 kW power and 100 mm out of focus. The scanning speed is 7000 mm/min and the samples are natural cooling in air. The surface of the specimen was finely polished to avoid the effect of surface roughness before x-ray diffractometer (XRD) measurement. The phase composition and morphologies of coatings were analyzed by XRD and scanning electron microscopy (SEM, JSM-6460, Japan), respectively.

Microhardness of TiB_2-$TiC_{0.3}N_{0.7}$ based composite coatings was measured by a Vickers tester (HX-1000, Shanghai, P.R. China) with 0.1 kg applied load and a dwell time of 40 s. The microhardness value was the average value of 10 measurement points in the middle of cross section of coatings. The cross section of coatings was polished before indentation. The distance between two indentations was at least three times of the diagonal to prevent stress field effect from the nearby indentation.

2.4 Weibull Distribution

Weibull distribution, which describes the broad and dispersive distribution of microhardness values for brittle ceramic material, is used to analyze the microhardness values of TiB_2-$TiC_{0.3}N_{0.7}$ based coatings. The Weibull distribution of two parameters is given as (Ref 19):

$$F(x) = 1 - \exp\left[-\left(\frac{x}{\eta}\right)^m\right] \quad \text{(Eq 1)}$$

where $F(x)$ is the cumulative density probability function, x is the selected microhardness value, η is the characteristic value and m is the Weibull modulus which reflects the dispersity of data in the distribution. The scale parameter η gives 63.2% of the cumulative density. Equation 1 can be transformed as follows:

$$\ln[-\ln(1 - F(x))] = m[\ln(x) - \ln(\eta)] \quad \text{(Eq 2)}$$

Therefore, a plot for $\ln[-\ln(1 - F(x))]$ versus $\ln(x)$ will be a linear relation if the Weibull modulus is suitable. The function of $F(x) = \frac{i}{n+1}$ is assumed with the data arranged in ascending order. The n in $F(x) = \frac{i}{n+1}$ is the total number of data points and i is the corresponding ordinal number (Ref 19, 20).

2.5 Electrochemical Measurements

The potentiodynamic polarization curves of coatings prepared by RPS with different composition powder were studied using a PARSTAT 2273 electrochemical system. Working electrode with 11 mm diameter was used in the electrochemical test. A high-density graphite electrode and a saturated calomel electrode (SCE) were used as the counter and reference electrodes, respectively. To imitate the seawater environment, 3.5 wt.% NaCl solution (cheap

and obtainable easily) was used as electrolyte. Potentiodynamic polarization tests were carried out from the initial potential of −1.4 V up to final potential of 3 V with scan rate of 0.05 V/s.

3. Results

3.1 Phase Composition and Microstructure

The phase composition of coatings is shown in Fig. 1. Samples A and B represent the coating deposited using compositions A and B powder, respectively. From the XRD results, it can be seen that the phase composition of two coatings is very similar. They are composed of main phases of TiB_2 and $TiC_{0.3}N_{0.7}$, minor phases of metallic binder Ni and Cr. The CoCr and TiO_2 phases are visible, but representing a smaller phase fraction. However, the Cr peak in XRD spectrum for the coating deposited using composition B powder is stronger than that of the coating deposited using composition A powder. The air is responsible for the production of titanium nitrides and titanium oxides. The TiB_2 phase is formed due to the reaction between the Ti and B_4C powder during the course of spraying. The reaction course during spraying has been discussed in detail in our previous research (Ref 20).

Figure 2 shows the morphology of spray-dried Ti-Cr-B_4C powder. It is very clear that the powder prepared by spray-drying is spherical with relatively uniform particle size. Figure 3 shows the micrographs of the coating deposited by RPS using composition A powder. The morphologies of the coating deposited by RPS using composition B powder and the coating with laser surface treatment are shown in Fig. 4. The coatings possess the lamellar structure and well bond with each other. It can be seen that the partially top coating (upper with arrow mark) in Fig. 4(a), which has been processed by laser scanning on the surface, is much denser than plasma sprayed coating. Some pores and non-melted particles

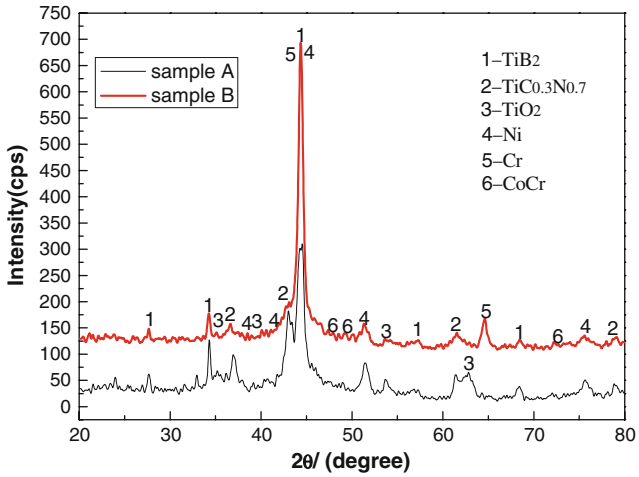

Fig. 1 XRD analysis of composite coatings

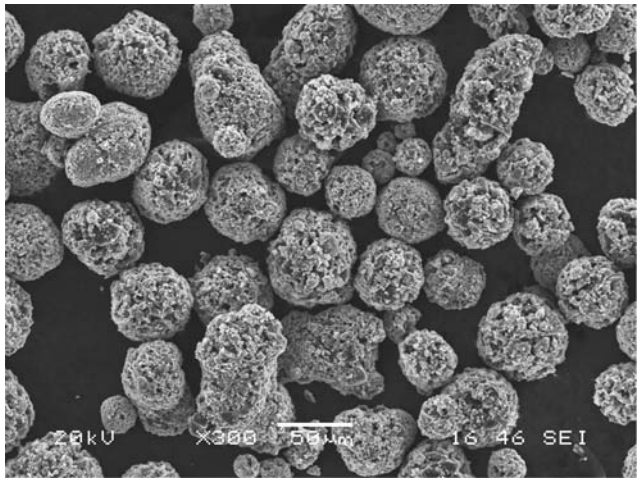

Fig. 2 SEM morphology of spray-dried powder

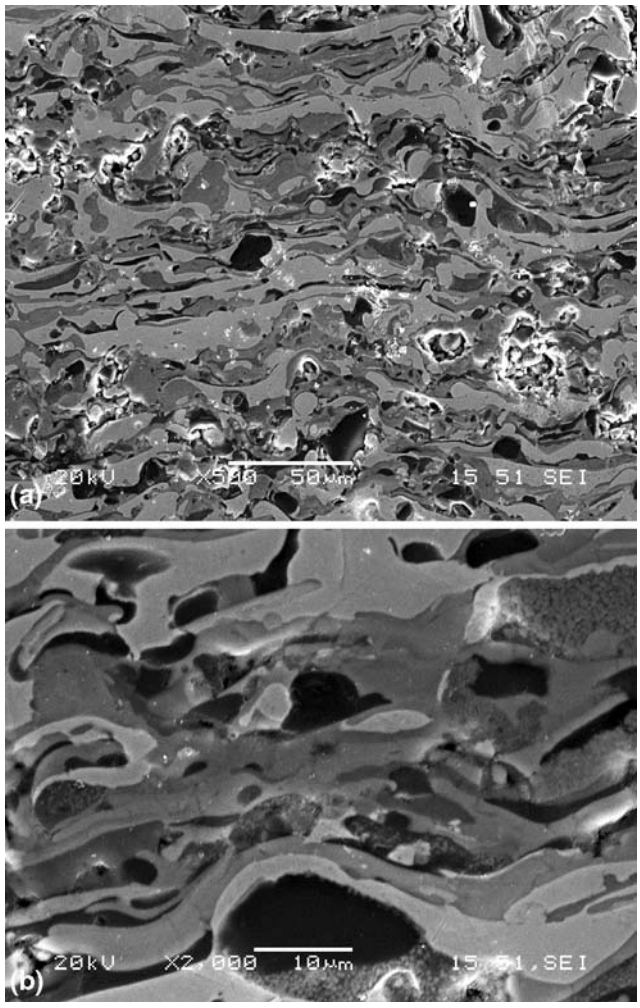

Fig. 3 SEM morphologies of the coating deposited using composition A powder: (a) low magnification; (b) high magnification

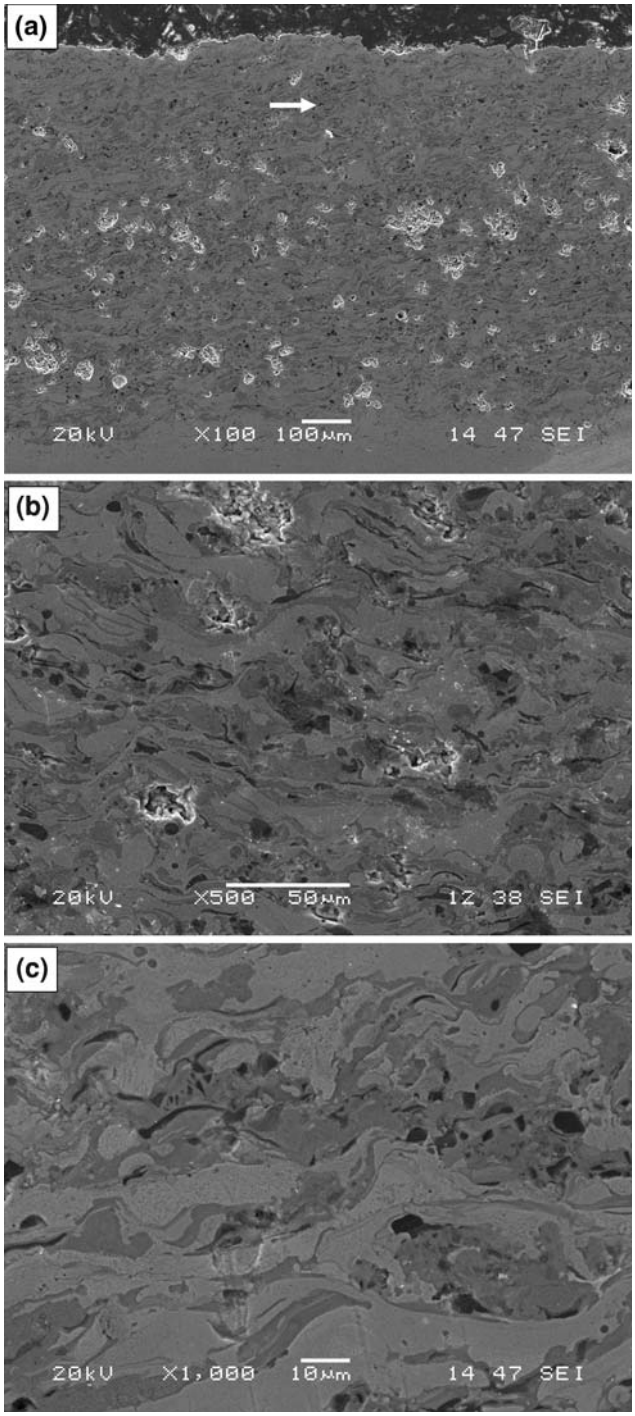

Fig. 4 SEM morphologies of the coating deposited using composition B powder. (a) The whole morphology of the plasma sprayed and laser treated coating; (b) partial enlarged micrograph of the plasma sprayed coating; (c) partial enlarged micrograph of the coating with laser surface treatment

decrease significantly after laser surface treatment (Fig. 4b, c).

There are mainly three different grey levels (regions 1, 2, and 3) in the top coating (Fig. 5). Combining the EDS

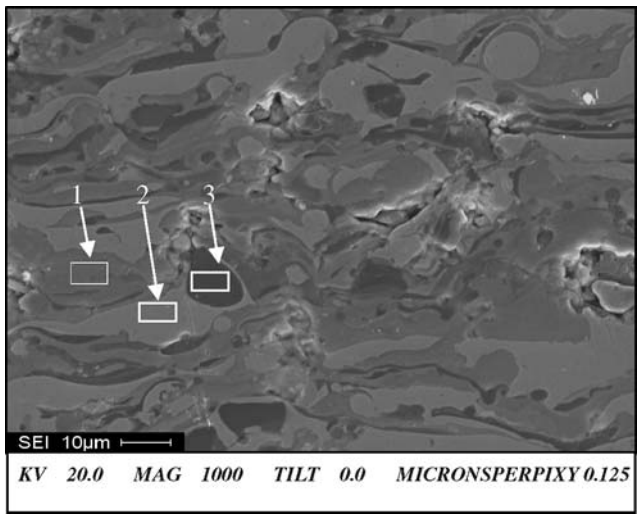

Fig. 5 EDS analysis of the plasma sprayed coating deposited using composition A powder

Table 2 Element analysis of EDS

District:	1	2	3
Element, wt.%			
Ti	37.18	7.64	8.28
B	36.44	11.95	80.70
C	5.07	4.69	7.89
N	9.17	4.18	2.09
O	11.01	2.35	0.44
Ni	0.52	47.05	0.27
Cr	0.45	20.27	0.23
Co	0.16	1.87	0.10

(Table 2) and XRD analyses, the composition of region 1 (grey) is main phases of TiB_2, $TiC_{0.3}N_{0.7}$ and a small fraction of TiO_2. The composition of region 2 (light grey) is main phases of metallic binder Ni, Cr and a little CoCr. In addition, the composition of region 3 (dark) is main phases of TiB_2 and a small fraction of $TiC_{0.3}N_{0.7}$. Compared with the cross-section micrographs of plasma sprayed coating (Fig. 3b) and the plasma sprayed coating with laser surface treatment (Fig. 4c), it can be seen that the phase distribution in the two coatings changes insignificantly. Several phases exist in both coatings according to the EDS analysis.

Figures 6 and 7 show the elements distribution on the cross section of the plasma sprayed coating and the coating with laser surface treatment (deposition using composition B powder), respectively. It can be concluded that the elements distribution are consistent with the EDS analysis in Fig. 5. The element B distributes mainly in dark region whereas Ni and Cr elements distribute primarily in light grey region. Most of the Ti, C, N and O elements disperse in grey area. It is very similar in elements distribution for the plasma-sprayed coating and the coating with laser treatment. According to our previous XRD analysis (the same phase composition) of the plasma

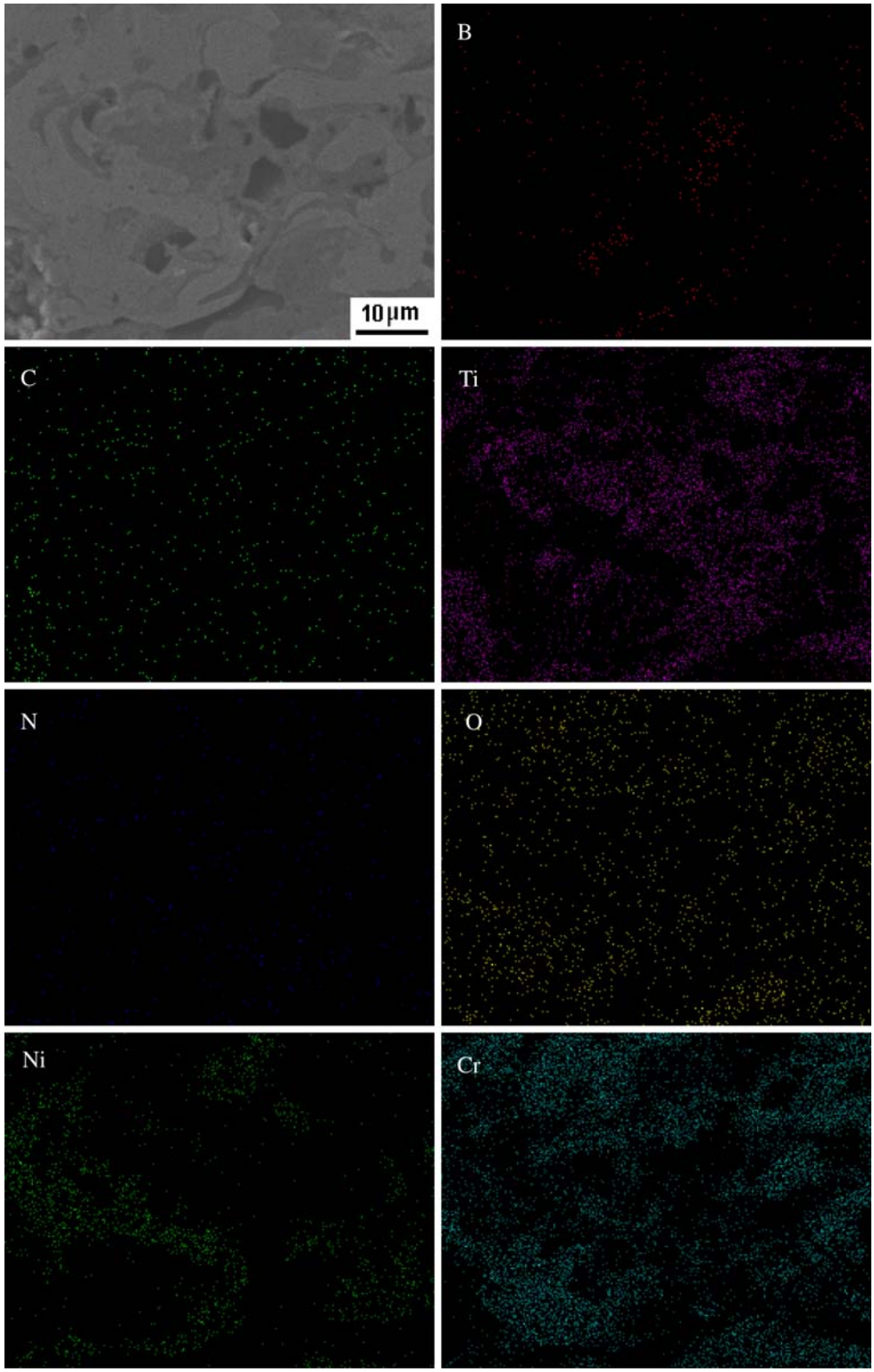

Fig. 6 The elements distribution on the cross section of plasma sprayed coating

sprayed coating and the coating with laser surface treatment using Ti-B_4C-Co spray-dried powder as well as the elements distribution in this study for the plasma sprayed coating and the coating with laser surface treatment, it can be inferred that the coating after laser surface treatment may not change the phase composition of the plasma-sprayed coatings deposited using Ti-B_4C systematic powder (spray-dried).

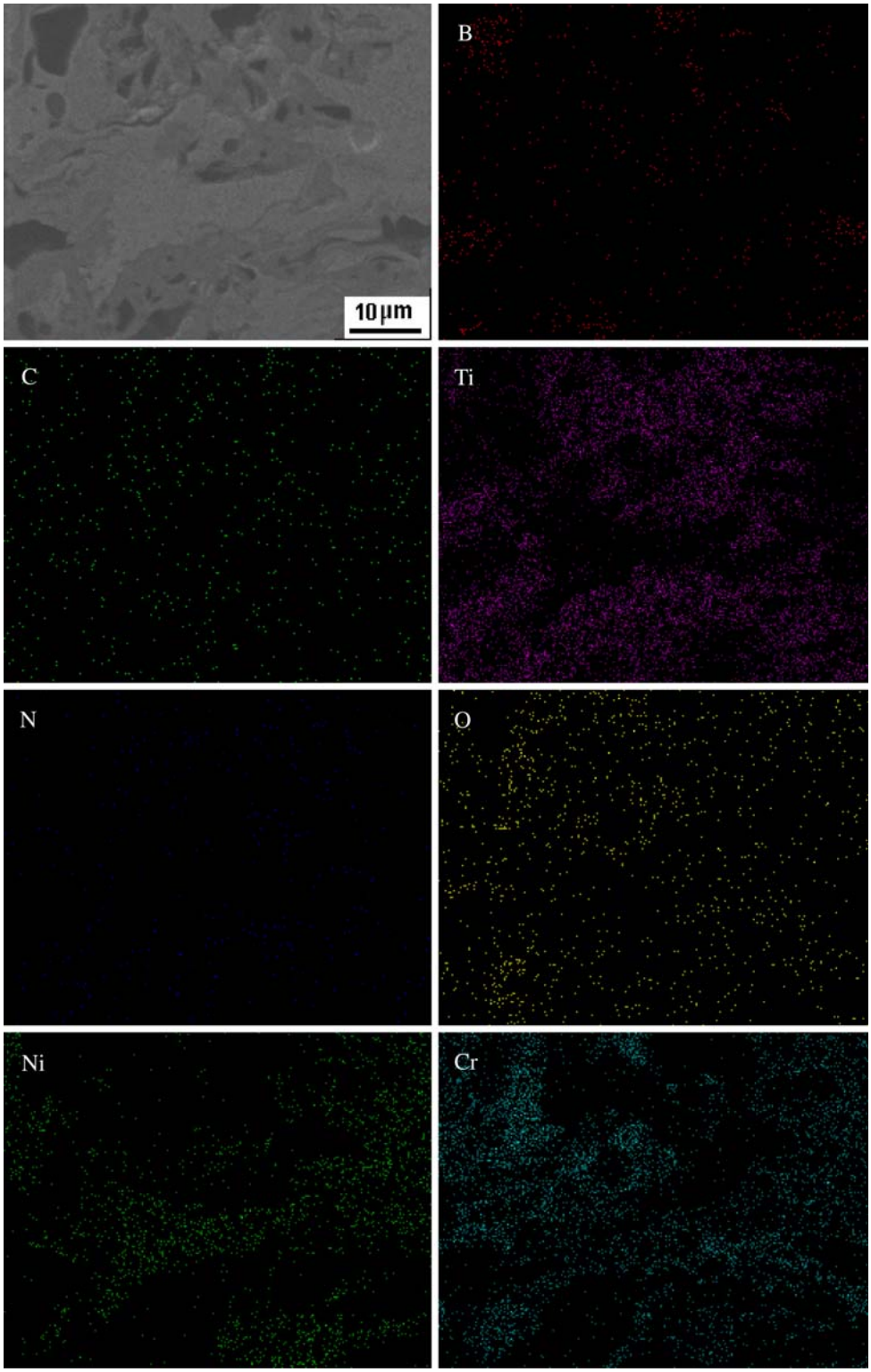

Fig. 7 The elements distribution on the cross section of the coating with laser treatment

3.2 Vickers Microhardness, Weibull Distribution and Polarization Curves

Table 3 shows the mean, minimum, maximum and standard error of Vickers microhardness for the cross section of coatings. A and A (L) represent the coating deposited using composition A powder and the coating processed by laser surface treatment, respectively. It is clear that the average Vickers microhardness value of

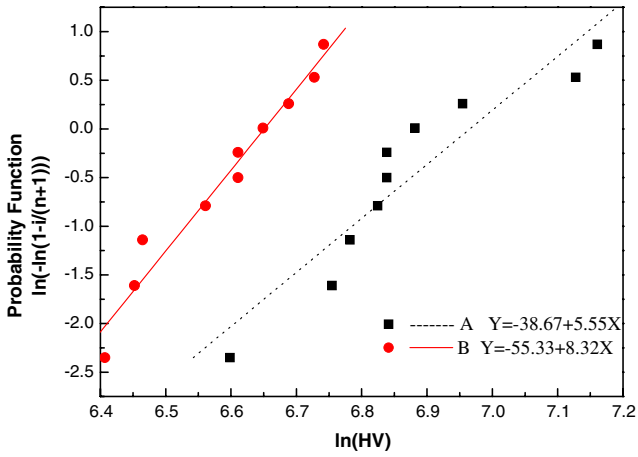

Fig. 8 The Weibull distribution of Vickers microhardness

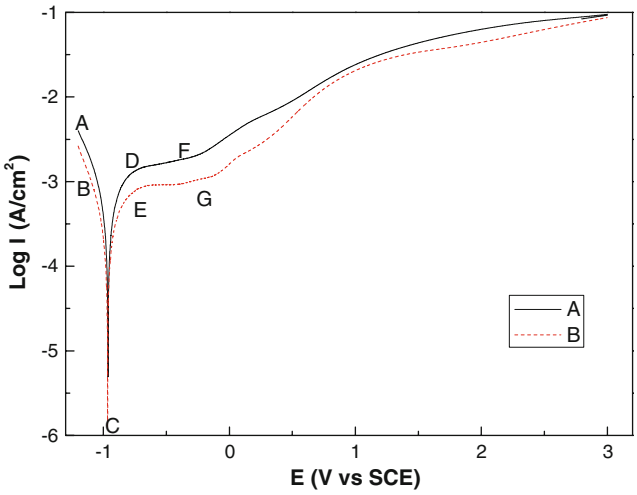

Fig. 9 Polarization curves of coatings

Table 3 Vickers microhardness of coatings at 0.1 kg

Sample	Mean	Min	Max	SE
A	982	734	1288	54
B	733	606	847	27
A (L)	1090	772	1818	113
B (L)	930	599	1226	64

Table 4 Summary of the results obtained from the Weibull distribution plots

Sample	Weibull modulus, m	Error	Hardness range in HV	ln (HV)
A	5.55	0.38	734-1288	6.60-7.16
B	8.32	0.21	606-847	6.41-6.74

each coating processed by laser surface treatment is higher than that of each reactive plasma sprayed coating. Furthermore, the mean Vickers microhardness value of the coating deposited using composition A powder is higher than that of the coating deposited using composition B powder.

The Weibull plot of the Vickers microhardness values on the cross section of coatings deposited by RPS using different composition powder at 0.1 kg applied load and their linear fit are shown in Fig. 8. The detailed information supplied by the figure is summarized in Table 4. Both of the Weibull modulus values are suitable to show a satisfactory distribution. Due to the low modulus corresponding to a high variability in the microhardness measurement, the measured microhardness values of the coating deposited using composition B powder show a smaller dispersion than that of the coating deposited using composition A powder.

The cathodic and anodic polarization curves corresponding to the coating deposited by RPS using compositions A and B powder are shown in Fig. 9. Curves AC and BC in the graph are cathodic polarization curves of coatings. Contrarily, curves CD and CE belong to anodic polarization curves. The corrosion current increases with the increment of potential in these regions. It indicates that these regions are active regions which correspond to the solution of surface materials. Both coatings have passive regions, shown in curves DF and EG. The corrosion current of the coating deposited using composition B powder is smaller than that of the coating deposited using composition A powder.

4. Discussion

4.1 The Influence of Powder Preparation Method on the Phase Composition of Coatings

Compared with the phase composition of coatings (predominant TiN and TiB_2) deposited by RPS using similar mixed powder (Ti, B_4C and Cr powder) in the previous research (Ref 20), some interesting things happened in this study. $TiC_{0.3}N_{0.7}$ phase appears instead of TiN phase in the phase composition of coatings. Ti(C, N) phase has a face center cubic (fcc) type NaCl structure, similar to the TiN structure with a partial substitution of atom N by atom C (Ref 21).

The different preparation method of powder for plasma spraying should be responsible for the phenomenon. The blended powder of Ti, Cr and B_4C after ball milling and screen separation was used for the deposition in the former study (Ref 20). In this research, the powder of Ti, Cr and B_4C for thermal spraying was blended, spray-dried, and then screen separated. The spray-dried powder, which contacts with each other tightly, is advantageous to the reaction and decreases the oxidation of Ti powder during spraying. The bond strength of blended powder is weaker than that of the spray-dried powder, which is very helpful to the reaction between Ti and B_4C powder. The blended powder of Ti and B_4C will be separated under high pressure of carrier gas due to their large density difference. The main reaction is between the Ti powder and N_2 in the atmosphere during the course of spraying. Therefore, the TiC phase generates more in the coating deposited using

spray-dried powder than that of the coating deposited using blended powder due to their better bond strength of Ti and B_4C. The TiC and TiN phases can interdiffuse to create Ti(C, N) phase during spraying due to their similar structure and high activity at high temperature.

4.2 The Influence of Cr Addition in the Thermal Spray Powder on the Microstructure of Coatings

It is obvious that the coating deposited by RPS using composition B powder (Fig. 4b) is much denser than that of the coating deposited using composition A powder (Fig. 3a) at the same magnification. The addition of Cr in the thermal spray powder should be responsible for this phenomenon. First, relatively low melting point of Cr powder can melt adequately at high temperature during RPS. The dispersive liquid Cr fills in the pores formed during the course of spraying and enhances the coating density very much. Second, the Cr powder, as a metallic binder, can improve the wetting property of ceramic phases of TiB_2 and $TiC_{0.3}N_{0.7}$ formed in situ. It enhances the bond strength of ceramic phases in the coating and decreases the separation of fragile ceramic phases. Third, the metal Cr in the coating can increase the toughness of TiB_2-$TiC_{0.3}N_{0.7}$ based composite coating. It is effective to hinder the formation of pores and crack propagation during the spraying (Ref 14).

However, the addition of Cr in the thermal spray powder decreases the Vickers microhardness on the cross section for the reactive plasma sprayed coatings. The mean Vickers microhardness value of the coating deposited by RPS using the composition A powder is 982 ± 54 $HV_{0.1}$, which is higher than that of the coating deposited by RPS using the composition B powder (733 ± 27 $HV_{0.1}$). The microhardness of metal Cr in the coating is much lower than that of the ceramic phases, such as TiB_2 and $TiC_{0.3}N_{0.7}$. It can affect the mean Vickers microhardness value of coatings to some extent. However, according to higher Weibull module obtained from the linear fit, the measured Vickers microhardness values of the coating deposited using composition B powder show a smaller dispersion than that of the coating deposited using composition A powder. This is shown that the Cr addition in the thermal spray powder homogenizes the phase distribution of ceramic-based coatings and decreases the partially conglomeration of hard phases. It may enhance the wear and corrosion resistance of the composite coating significantly.

4.3 Laser Surface Treatment for the Reactive Plasma Sprayed Coatings

As shown in Fig. 4(a), the top coating with laser surface treatment is much denser than the reactive plasma sprayed coating. It is very clear that most pores in the coating disappear after laser processing (Fig. 4b, c). Furthermore, the mean Vickers microhardness value also increases to 1090 ± 113 $HV_{0.1}$ (11% higher than its plasma sprayed coating) for the coating deposited by RPS using composition A powder and 930 ± 64 $HV_{0.1}$ (27% higher than its plasma sprayed coating) for the coating deposited by RPS using composition B powder after laser scanning on the surface of coatings. Due to high power of CO_2 laser, the reactive plasma sprayed coatings may remelt under laser heating. The gas in the pores of the coating floats to the surface and eliminates during the solidification of the coating. It is reasonable that the coating with laser surface treatment is denser than that of the plasma sprayed coating. In addition, the Vickers microhardness increases with the decrease of pores and other drawbacks (crack or unmelted particles) through laser processing.

However, after laser surface treatment of the reactive plasma sprayed coatings, the increased range of the Vickers microhardness value of the coating deposited using composition B powder is higher than that of the coating deposited using composition A powder (27% versus 11%). The main reason is the addition of Cr in the thermal spray powder. The relatively low melting point of metal Cr than ceramic phases in the coating can melt and flow sufficiently during the laser heating. It can improve the wettability of the ceramic phases in reactive plasma sprayed coating. These ceramic phases in the coating will bond better after laser surface treatment for the coatings. Unfortunately, there are some cracks in both laser surface treatment coatings due to quickly cooling velocity and relatively high content of ceramic phases. The mismatch of CTE for the ceramic phases and metal phases can also lead to the formation of crack during the laser scanning.

4.4 The Influence of Cr Addition in the Thermal Spray Powder on the Corrosion Resistance Property of Coatings

It is very obvious that typical passive region for both coatings (curves DF and EG) are found in the graph (Fig. 9). The protective film generates in passive region. However, it is pierced with the increment of potential. The currents increase very slowly with the increment of potential in passive region due to the protective film hindering the penetration of corrosion medium in 3.5 wt.% NaCl electrolyte. Comparing the corrosion resistance property of coatings deposited by RPS using different composition powder, it can be concluded that the coating deposited using the composition B powder possesses better corrosion resistance in 3.5 wt.% NaCl electrolyte due to its smaller corrosion current.

There are mainly two reasons for the phenomenon. First, the coating deposited by RPS using the powder with Cr addition is denser. Less pores and cracks can hinder the penetration of corrosion medium well. Second, Cr as a corrosion resistance element has been widely used in the industry due to its high chemical homogeneity and high chemical reactivity (Ref 22). Alloys with Cr element show high corrosion resistance due to formation of Cr-enriched passive films (Ref 23). The metal Cr existed in the composition of the coating can also work as the same way in the 3.5 wt.% NaCl electrolyte.

5. Conclusions

In summary, TiB_2-$TiC_{0.3}N_{0.7}$ based composite coatings were successfully prepared using RPS. The coating becomes dense whereas the Vickers microhardness values decrease a little with the Cr addition in the thermal spray powder. The reactive plasma sprayed coatings after laser surface treatment may obtain partially remelted coatings with denser microstructure and higher microhardness value. In addition, the corrosion resistant property of the coating deposited by RPS with Cr addition in thermal spray powder is better. However, the wear resistance property and corrosion mechanics of different stage in electrolyte for the coating should be investigated in the future. Solving methods for decreasing the crack formation in the coating after laser surface treatment also need to be studied further.

Acknowledgments

The authors are grateful to Mr. Wang for coatings deposition and XRD analysis by Mr. H. B. Han in the instrumental analysis center of Shanghai Jiaotong University. This work was supported by the Plan of Dawn from education committee of Shanghai Municipality and the Academic Leader Plan from Science and Technology Commission of Shanghai Municipality. The authors are also thankful for the hard work of editors and reviewers on the paper.

References

1. S.J. Bull, D.G. Bhat, and M.H. Staia, Properties and Performance of Commercial TiCN Coatings. Part 1: Coating Architecture and Hardness Modelling, *Surf. Coat. Technol.*, 2003, **163-164**, p 499-506
2. Z. Mao, J. Ma, J. Wang, and B. Sun, Properties of TiN-Matrix Coating Deposited by Reactive HVOF Spraying, *J. Coat. Technol. Res.*, 2009, **6**, p 243-250
3. Y. Tsunekawa, M. Okumiya, T. Kobayashi, M. Okuda, and M. Fukumoto, Chromium-Nitride In Situ Composites with a Compositional Gradient Formed by Reactive DC Plasma Spraying, *J. Therm. Spray Technol.*, 1996, **5**, p 139-144
4. A. Singh and N.B. Dahotre, Laser In Situ Synthesis of Mixed Carbide Coating on Steel, *J. Mater. Sci.*, 2004, **39**, p 4553-4560
5. A. Anal, T.K. Bandyopadhyay, and K. Das, Synthesis and Characterization of TiB_2-Reinforced Iron-Based Composites, *J. Mater. Process. Technol.*, 2006, **172**, p 70-76
6. I. Ozdemir, I. Hamanaka, M. Hirose, Y. Tsunekawa, and T.M. Okumiya, In Situ Formation of Al-Si-Mg Based Composite Coating by Different Reactive Thermal Spray Processes, *Surf. Coat. Technol.*, 2005, **200**, p 1155-1161
7. J.F. Li, H. Liao, B. Normand, C. Cordier, G. Maurin, J. Foct, and C. Coddet, Uniform Design Method for Optimization of Process Parameters of Plasma Sprayed TiN Coatings. *Surf. Coat. Technol.*, 2003, **176**, p 1-13
8. E. Galvanetto, F.P. Galliano, F. Borgioli, U. Bardi, and A. Lavacchi, XRD and XPS Study on Reactive Plasma Sprayed Titanium-Titanium Nitride Coatings, *Thin Solid Films*, 2001, **384**, p 223-229
9. L. Xiao, D. Yan, J. He, L. Zhu, Y. Dong, J. Zhang, and X. Li, Nanostructured TiN Coating Prepared by Reactive Plasma Spraying in Atmosphere, *Appl. Surf. Sci.*, 2007, **253**, p 7535-7539
10. F. Kikkawa, H. Tamura, and K.-i. Kondo, Ti-B-C Composite Coating Produced by Electrothermally Exploded Powder-Spray Technique, *J. Therm. Spray Technol.*, 2006, **15**, p 92-96
11. M.A. Capano, A.A. Voevodin, J.E. Bultman, and J.S. Zabinski, Pulsed Laser Deposition of Titanium-Carbonitride Thin Films, *Scr. Mater.*, 1997, **36**, p 1101-1106
12. B. Du, S.R. Paital, and N.B. Dahotre, Phase Constituents and Microstructure of Laser Synthesized TiB_2–TiC Reinforced Composite Coating on Steel, *Scr. Mater.*, 2008, **59**, p 1147-1150
13. V.N. Zhitomirsky, S. Wald, M. Factor, L. Rabani, D. Zoler, S. Cuperman, C. Bruma, and I. Roman, WC–Co Coatings Deposited by the Electro-Thermal Chemical Spray Method, *Surf. Coat. Technol.*, 2000, **132**, p 80-88
14. D.A. Stewart, P.H. Shipway, and D.G. McCartney, Microstructural Evolution in Thermally Sprayed WC–Co Coatings: Comparison Between Nanocomposite and Conventional Starting Powders, *Acta Mater.*, 2000, **48**, p 1593-1604
15. Q. Yang, T. Senda, and A. Ohmori, Effect of Carbide Grain Size on Microstructure and Sliding Wear Behavior of HVOF-Sprayed WC–12% Co Coatings, *Wear*, 2003, **254**, p 23-34
16. J.M. Guilemany, J.M. Miguel, S. Vizcaino, and F. Climent, Role of Three-Body Abrasion Wear in the Sliding Wear Behaviour of WC–Co Coatings Obtained by Thermal Spraying, *Surf. Coat. Technol.*, 2001, **140**, p 141-146
17. G.Y. Liang, T.T. Wong, J.M.K. MacAlpine, and J.Y. Su, A Study of Wear Resistance of Plasma-Sprayed and Laser-Remelted Coatings on Aluminium Alloy, *Surf. Coat. Technol.*, 2000, **127**, p 233-238
18. G. Xie, X. Lin, K. Wang, X. Mo, D. Zhang, and P. Lin, Corrosion Characteristics of Plasma-Sprayed Ni-Coated WC Coatings Comparison with Different Post-Treatment, *Corros. Sci.*, 2007, **49**, p 662-671
19. H. Zhou, F. Li, B. He, J. Wang, and B.-d. Sun, Air Plasma Sprayed Thermal Barrier Coatings on Titanium Alloy Substrates, *Surf. Coat. Technol.*, 2007, **201**, p 7360-7367
20. Z. Mao, J. Ma, J. Wang, and B. Sun, The Effect of Powder Preparation Method on the Corrosion and Mechanical Properties of TiN-Based Coatings by Reactive Plasma Spraying, *Appl. Surf. Sci.*, 2009, **255**, p 3784-3788
21. G. Levi, W.D. Kaplan, and M. Bamberger, Structure Refinement of Titanium Carbonitride (TiCN), *Mater. Lett.*, 1998, **35**, p 344-350
22. K. Hashimoto, K. Osada, T. Masumoto, and S. Shimodaira, Characteristics of Passivity of Extremely Corrosion-Resistant Amorphous Iron Alloys, *Corros. Sci.*, 1976, **16**, p 71-76
23. H. Habazaki, H. Ukai, K. Izumiya, and K. Hashimoto, Corrosion Behaviour of Amorphous Ni–Cr–Nb–P–B Bulk Alloys in 6M HCl Solution, *Mater. Sci. Eng. A*, 2001, **318**, p 77-86